ROGUE WAVES

G. Hocking[1] and C. Please[2]

Industry Representative

Thama Duba, Durban University of Technology, Durban

Study group participants

M. Kennealy and K. Born

Abstract

For the safe passage of ships it is critical to avoid weather and ocean conditions that may endanger, damage or even sink them. One serious, potential problem is that of "rogue waves", commonly also called "freak", "monster" or "abnormal" waves. These are waves whose amplitude is unusually large for a given sea state. In this report we consider several possible mechanisms for the formation of rogue waves, and provide some references that consider the issue in more detail. We also revisit an analysis of nonlinear wave interactions that may explain the formation of these waves in the absence of other factors such as currents or variable bottom topography.

Figure 1: The Great Wave off Kanagawa, *H. O. Havemeyer Collection, Bequest of Mrs. H. O. Havemeyer, 1929*

[1] Murdoch University, Western Australia, Australia. *email: G.Hocking@murdoch.edu.au*
[2] University of Oxford, United Kingdom. *email: Colin.Please@maths.ox.ac.uk*

Figure 2: Photograph of what is believed to be a rogue wave. It is difficult to get a scale on the size of this wave.

1 Introduction

For the safe passage of ships it is critical to avoid weather and ocean conditions that may endanger, damage or even sink them. One serious, potential problem is that of “rogue waves”, commonly also called “freak”, “monster” or “abnormal” waves. These are waves whose amplitude is unusually large for a given sea state. A very well known historical depiction of such a wave is given in Figure 1, a woodblock print published in the early 1800s by Katsushika Hokusai. McAllister et. al. [5] have produced a wave in a wave-tank that looks very much like this print. One of the few photographs of such a phenomena in the ocean is shown in Figure 2, although it is difficult to get perspective in this photograph to see the physical size of this wave. Descriptions of these waves have a long history in sea folklore, but at times there has been considerable scepticism about their existence.

Reports suggest that these waves appear and disappear suddenly and unexpectedly. Trying to identify situations where they might occur would be very helpful in the planning of shipping routes. The Study Group was asked to explore mechanisms that might create rogue waves and to consider if some general rules could be found that might explain where and when they might occur.

There is a vast literature on mathematical modelling approaches to wave behaviour relevant to the sea, and a more authoritative review is given by Dysthe et al. [4]. There is a considerable subset of this literature that is focussed on different aspects of rogue wave behaviour and this report presents some of those ideas and some analysis of particular aspects. We note that there are other physical situations where rogue waves can apparently occur including optical fibres, the atmosphere and plasmas, but we do not consider these further.

There is no precise definition of a rogue wave but a common rule is that such a wave is larger than the general surrounding wave field. A slightly more formal definition is that a rogue wave has

$$\frac{\eta_c}{H_{1/3}} > 1.2 \qquad \text{or} \qquad \frac{H}{H_{1/3}} > 2 \tag{1}$$

where the particular wave has a crest height η_c and a wave height H, and $H_{1/3}$ is the significant wave height; the mean wave height (trough to crest) of the highest third of the waves, see [1]. Example wave records can be found in Dysthe et. al. [4].

1.1 Possible causes of rogue waves

The literature and discussion in the study group identified a number of physical mechanisms that might cause such waves. These are;

- **Weather conditions**

  Various weather conditions and sea states, particularly very high seas, seem to be correlated with rogue wave observations from ships, but this may simply be that the waves are already large and so larger waves are ones that cause damage while a rogue wave in smaller seas may not be noticed. Rogue waves may be created due to relatively isolated phenomena that move to induce a large local wave. Examples could be moving low pressure systems, hurricanes, cyclones or tornadoes.

- **Wave-current and current-current interactions**

  When wind acts against a current the waves that are produced can be much larger than when no current is present. It would be interesting to consider the effect of currents especially in situations where the current changes direction when it meets another current. Whether such situations might produce rogue waves is not clear.

- **Topography**

  The bottom topography of the ocean, such as at the edge of the continental shelf, can sometimes create a focussing or amplification of waves. For example the converging Bristol Channel amplifies the bore in the Severn River, while the topography near the coast of Portugal leads to monster waves used by surfers. In these two cases the waves are shallow-water waves and only become large when they travel in the direction of decreasing depth. It is believed that rogue waves can occur in very deep water so the waves would need to travel large distances if this were the mechanism. If this were a mechanism, these waves would tend to occur often in the same locations.

- **Wave-wave interactions**

  Much of the modelling to predict rogue waves considers long waves. Such waves are, to lowest order, simple linear waves. One approach is to note that a number of different wave trains, perhaps travelling in different directions, may simply add together to create a large isolated wave. Such waves would exist for extremely short times and would require all of the factors to align at just the right moment. It would seem unlikely that this is the mechanism. A second possibility, that has received enormous theoretical interest, is that over long times a very small nonlinear interaction between the waves may allow some waves to grow at the expense of others. These nonlinear phenomena can create solitons which are isolated in space and have large amplitude. Such behaviour has been exploited in, for example, optical devices. It is not obvious if such behaviour would give a single sea wave since it predicts a packet of many waves interacting and hence might be observed as a group of large waves rather than a single, isolated wave.

This is not an exhaustive list but gives many of the factors that might be considered. For each of them it would appear that examining a model of the behaviour might allow predictions to be made of the probability of a rogue wave event.

In this report we will concentrate on the modelling that has been done on the phenomena of long-time nonlinear wave-wave interactions where the waves are travelling in a single direction. Our motivation is to see if there are particular physical properties of the wave trains that control the possible creation of larger waves with a soliton-type structure.

1.2 Where have rogue waves been reported?

The group thought there may be a clue to the mechanisms behind rogue waves from their reported locations. For example, do they occur in strong currents or near the continental shelf more often than elsewhere? Initially these waves were reported by sailors who survived disasters and wrote that their ships had been hit by phenomenally large waves, "walls of water", that came from nowhere and destroyed their ship. Because such waves were very rare events and, one suspects, most sailors who observed them perished in the subsequent disaster, these were treated as folklore by most people. Not until 1995, when the Draupner oil platform in the North Sea with sensors collecting data about waves was hit by a 29m wave, was such a wave observed in sufficient detail for the phenomena to be treated seriously and efforts made to understand their source. Since that time research to observe rogue waves has increased and both satellite images and sensors on large ships have allowed more detailed measurement of how many waves occur.

In Figure 3 the red pins denote the approximate positions of all the rogue waves observed around the world (see [6]). A more detailed map is given in Dysthe et. al. [4]. We can see in more detail these positions by looking just in the North Atlantic (see Figure 4 which shows the positions of reported rogue waves [6] and the size of the ocean currents [7]) and we note that those observations off the coast of North America may be associated with the Gulf Stream current that travels north. We also note that many rogue waves are seen off the western coast of Britain, but there is not a large current there. In Figure 5 the reported rogue wave positions and the ocean currents are shown for the south west of the Indian Ocean. The red pin marked "13" indicates where a total of 13 rogue waves have been observed while the red pin marked "12" indicates the position of 12 rogue waves. Note that in this figure there appears to be some relation between the number of rogue waves and the strong coastal currents.

These data from a long period of time give some idea of where rogue waves occur. However, great care is needed in interpreting this because much of it was collected when the chances of surviving a rogue wave were very small and the data is probably vastly skewed to record rogue waves in only a small sub region of the globe because observations are almost entirely dominated by data in shipping routes. Given the picture emerging

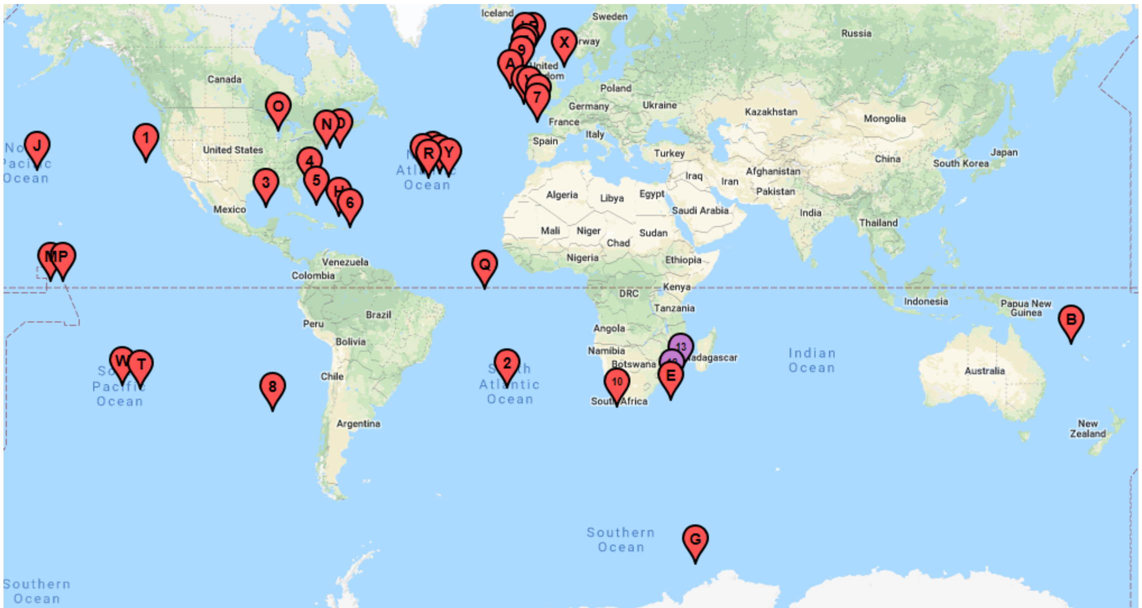

Figure 3: Approximate location of recorded rogue waves around the World (see [6]).

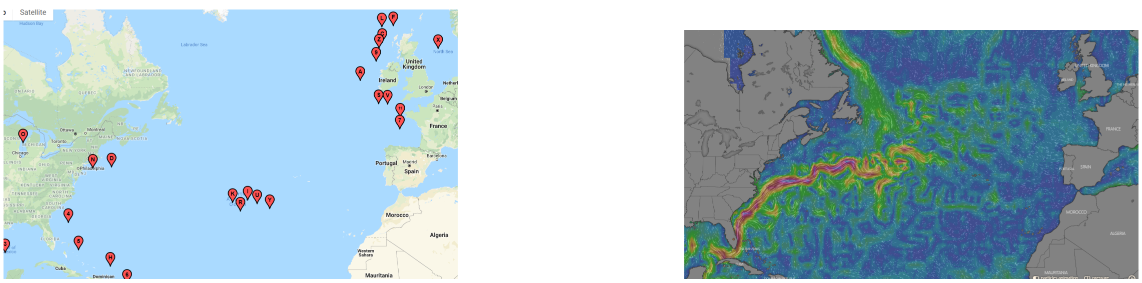

Figure 4: Locations of rogue wave sightings, [6] and a heat map of the ocean currents in the same region ([7]). Note that some reports simply say "North Atlantic" and these are indicated by a red pin in the centre of the Atlantic.

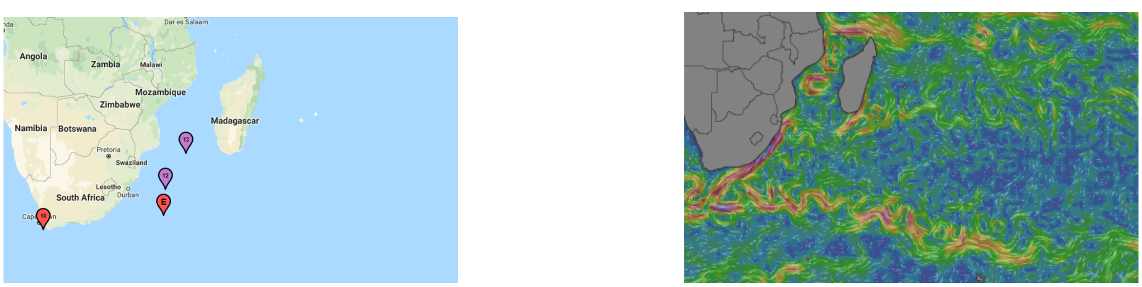

Figure 5: Position of rogue wave observations [6] and a vector field of the ocean currents in the South Western Indian Ocean ([7]). Red pins 13 and 12 each indicate many rogue wave observations.

from this diagram, there is no clear pattern to the location of these waves and so although this provides an interesting picture of the distribution of waves, it does not help in finding the cause or causes.

2 Modelling

We now consider mathematical modelling approaches that have been taken to explain the behaviour of a train of waves all travelling in the same direction and how very small nonlinear interactions might make a group of waves either grow in size, travel at a constant size or decay away. There are two main models that have been derived to explain such behaviour and these are:

- the nonlinear Schrödinger equation (NLSE)
- the Dysthe Equation (a Modified Schrödinger equation (MNLSE))

Let us consider how the NSLE arises and an analysis that may tell us whether nonlinear wave interactions might lead to a rogue wave.

2.1 The equations for waves in deep water

We start by considering waves on an infinitely deep sea (with z being the vertical coordinate upwards) where the fluid motion is described by the irrotational flow of an inviscid, incompressible fluid with the wave surface given by $z = \eta(x, y, t)$ and conditions on the surface given by a kinematic condition (fluid particles on the surface remain on the surface) and a Bernoulli condition (the pressure of the air above the waves is uniform and constant). In that case, we can define a velocity potential $\phi(x, y, z, t)$ such that the velocity $\mathbf{v} = \nabla\phi$. The model is therefore

$$\nabla^2\phi = 0, \qquad -\infty < z < \eta(x,t), -\infty < x < \infty, t > 0 \tag{2}$$

subject to the dynamic condition that the pressure on the water surface must be atmospheric, i.e.

$$\phi_t = -\frac{1}{2}\left(\phi_x^2 + \phi_y^2 + \phi_z^2\right) - g\eta \quad \text{on} \quad z = \eta(x, y, t) \tag{3}$$

where g is the gravity constant, and the kinematic condition given by

$$\eta_t = \eta_x\phi_x + \eta_y\phi_y - \phi_z \quad \text{on} \quad z = \eta(x, y, t) \tag{4}$$

and finally a condition that there is no disturbance deep beneath the ocean, so that

$$\phi \to 0 \quad \text{as} \quad z \to -\infty. \tag{5}$$

This general wave problem is too difficult to completely solve analytically because it is highly nonlinear due to the quadratic terms in the dynamic (Bernoulli) condition and the fact the the surface $z = \eta(x, y, t)$ is *apriori* unknown. Therefore, we consider the long wavelength limit where the height of the waves is small compared to the length.

In what follows, we are essentially repeating the analysis of Dysthe [3] in deriving a nonlinear Schrödinger equation for deep water waves. We will not provide the full derivation, but give enough detail to provide an understanding of how the equations arise and more importantly what scaling has been used.

We will assume the waves to be two-dimensional and hence will ignore the lateral y-direction in our work so that we seek the behaviour of the potential function, $\phi(x, z, t)$ and surface elevation $\eta(x, t)$. Note that Dysthe included the full 3 dimensional equations.

In the case of long waves we consider k as the wavenumber of the waves and a as the amplitude where we will analyse in the case where the parameter $\varepsilon = ka$ is small. We introduce scales

$$x = \frac{1}{k}\hat{x}, \quad z = \frac{1}{k}\hat{z}, \quad t = \frac{1}{\sqrt{gk}}\hat{t}, \quad \phi = a\sqrt{\frac{g}{k}}\hat{\phi}, \quad \text{and} \quad \eta = a\hat{\eta}.$$

Putting these into the model, and dropping the hat notation for simplicity, we find that the non-dimensional potential still satisfies

$$\nabla^2\phi = 0, \qquad -\infty < z < \varepsilon\eta(x,t), -\infty < x < \infty, t > 0 \tag{6}$$

and the non-dimensional surface conditions are

$$\phi_t + \eta + \frac{\varepsilon}{2}\left(\phi_x^2 + \phi_z^2\right) = 0, \text{ on } z = \varepsilon\eta(x,t) \tag{7}$$

$$\eta_t + \varepsilon\phi_x\zeta_x - \phi_z = 0, \text{ on } z = \varepsilon\eta(x,t) \tag{8}$$

Progress can now be made by assuming the dependent variable can be expanded in the usual way and be written in the usual expanded forms

$$\begin{aligned} \phi &= \phi_0 + \varepsilon\phi_1 + \varepsilon^2\phi_2 + \ldots \\ \eta &= \eta_0 + \varepsilon\eta_1 + \varepsilon^2\eta_2 + \ldots . \end{aligned} \tag{9}$$

If we now consider the problem at each order of ε get the following problems: at order $O(1)$

$$\nabla^2\phi_0 = 0, \tag{10}$$

$$\text{with} \quad \phi_{0t} + \eta_0 = 0, \quad \text{on} \quad z = 0. \tag{11}$$

$$\text{and} \quad \eta_{0t} - \phi_{0z} = 0 \quad \text{on} \quad z = 0. \tag{12}$$

at order $O(\varepsilon)$

$$\nabla^2\phi_1 = 0, \tag{13}$$

$$\text{with} \quad \phi_{1t} + (\phi_{0z}\eta_0)_t + \eta_1 + \frac{1}{2}\left(\phi_{0x}^2 + \phi_{0z}^2\right) = 0, \tag{14}$$

$$\text{and} \quad \eta_{1t} + \phi_{0x}\eta_{0x} - \phi_{1z} - (\phi_{1z}\eta_0)_z = 0. \tag{15}$$

Note in deriving these we have had to take care when evaluating the boundary conditions on $z = \varepsilon\eta$, so that we have expanded to find that

$$\frac{\partial\phi(x,z,t)}{\partial t} = \frac{\partial}{\partial t}\left(\phi(x,0,t) + \varepsilon\eta(x,t)\frac{\partial\phi}{\partial z}(x,0,t) + \frac{\varepsilon^2\eta(x,t)^2}{2}\frac{\partial^2\phi}{\partial t^2}(x,0,z) + \ldots\right)$$

and then inserted (9) to then equate powers of ε.

These calculations can be continued with the model to higher orders, but we will not proceed further. The important fact is that we have correctly identified the required scalings and leading order equations.

The resulting equation becomes;

$$2i\left(\frac{\partial u_0}{\partial \bar{t}}+\frac{1}{2}\frac{\partial u_0}{\partial \bar{x}}\right)-\frac{\partial^2 u_0}{\partial \bar{t}^2}=4u_0\,|u_0|^2+\{\text{higher order terms}\} \tag{16}$$

This can be seen in the work of Dysthe [3], where the dimensional form of the equation is given as, using their notation,

$$2i\omega\left(\frac{\partial A}{\partial t}+v_g\frac{\partial A}{\partial x}\right)-\frac{\partial^2 A}{\partial t^2}=A\big(4k^4\,|A|^2+\{\text{higher order terms}\}\big) \tag{17}$$

where we have neglected y derivatives (since we are assuming two-dimensional waves) and A is the dimensional complex potential varying slowly with time scale εt and length scale εx. The quantity $\omega=\sqrt{kg}$, and $v_g=\sqrt{g/k}/2$ is the group velocity.

In order to proceed, we can now obtain the leading order solution. By inspection (or using separation of variables, or Fourier transforms) one can identify solutions of the form

$$\phi_0(x,z,t)=\frac{-iu_0}{\kappa}\exp(z\kappa)\exp\big(i(x\kappa-t\sqrt{\kappa})\big), \tag{18}$$

and for the surface shape, it follows that

$$\eta(x,t)=u_0\exp\big(i(x\kappa-t\sqrt{\kappa})\big). \tag{19}$$

for any constant κ, where u_0 may be complex, and we take linear sums of these waves and the real part of the resulting expression. For the problems of interest we consider the case where the nondimensional wavenumber κ is near unity. In this case this solution represents waves moving to the right with speed close to unity with amplitude nearly u_0. For $\kappa=1$ we have

$$\phi(x,z,t)=-iu_0\exp(z)\exp\big(i(x-t)\big), \tag{20}$$

and

$$\eta(x,t)=u_0\exp\big(i(x-t)\big). \tag{21}$$

At first-order then, we can see that (dropping the $^-$ for convenience)

$$\frac{\partial u_0}{\partial t}=-\frac{1}{2}\frac{\partial u_0}{\partial x}, \tag{22}$$

and substituting this into the time derivative term leads to $\frac{\partial^2 u_0}{\partial t^2}\approx\frac{1}{4}\frac{\partial^2 u_0}{\partial x^2}$ so that eventually we obtain the nonlinear Schrödinger equation

$$\frac{\partial u}{\partial t}+\frac{1}{2}\frac{\partial u}{\partial x}+\frac{i}{8}\frac{\partial^2 u}{\partial x^2}+\frac{i}{2}|u|^2u=0 \tag{23}$$

This equation is known to have a very special type of solution, namely a soliton, of the form

$$u(x,t)=\frac{\mathrm{e}^{it/2}}{\sqrt{2}}\operatorname{sech}\left(x-\frac{1}{2}t\right). \tag{24}$$

The exponential term in (24) represents an oscillation on this slow time scale, so that the soliton moves up and down as it progresses. The absolute value of this term is

$$|u(x,t)| = \frac{1}{\sqrt{2}} \left| \operatorname{sech}\left(x - \frac{1}{2}t\right)\right|, \tag{25}$$

and it is the behaviour of this quantity that we will analyse.

Firstly, notice that $u(x,t)$ may be complex, so taking u^* as the complex conjugate, we can write the conjugate equation as

$$\frac{\partial u^*}{\partial t} + \frac{1}{2}\frac{\partial u^*}{\partial x} - \frac{i}{8}\frac{\partial^2 u^*}{\partial x^2} - \frac{i}{2}|u|^2 u^* = 0. \tag{26}$$

Multiplying (23) by u^* and (26) by u, adding and then integrating from $-\infty$ to ∞ gives

$$\int_{-\infty}^{\infty} \frac{\partial(uu^*)}{\partial t} + \frac{1}{2}\frac{\partial(uu^*)}{\partial x} + i\frac{i}{8}\left(u^*\frac{\partial^2 u}{\partial x^2} - u\frac{\partial^2 u^*}{\partial x^2}\right) \mathrm{d}x = 0 \tag{27}$$

If we now note that u and u_x both approach zero as $x \to \pm\infty$, and that the second derivative terms can be integrated to $(u^* u_x - u u_x^*)_x$ this equation simplifies to show

$$\frac{\partial}{\partial t}\left(\int_{-\infty}^{\infty} |u|^2 \mathrm{d}x\right) = 0. \tag{28}$$

This is essentially an energy argument that says that the energy contained in the wave packet must remain constant.

We now consider allowing the form of u to vary slowly by assuming the form

$$|u(x,t)| = A(t)\operatorname{sech}\left(\frac{x - ct}{L(t)}\right) \tag{29}$$

where $A(0) = A_0$ and $L(0) = L_0$ are the initial amplitude and wavelength respectively. If we take the special case $A_0 = 1/\sqrt{2}$, $L_0 = 1$ we have the soliton. Using the energy argument we note that in general, if (29) were a solution, then for the energy to remain constant we require

$$L(t) = L_0 \left|\frac{A_0}{A(t)}\right|^2. \tag{30}$$

2.2 Nonlinear long-wave behaviour

Considerable analysis exists for the NLSE including many numerical methods. Here, however, we pursue the route taken by Cousins et al. [2], who sought an approximate solution to the NLSE with the aim of gaining insight into the general behaviour of the problem without extensive computations being necessary. The idea is to assume that the envelope of the wave will remain close in shape to a soliton but that its height and length may change. The procedure is to parametrise the solution, such as in (29), and then take integrals in x of the resulting NLSE to generate approximate ordinary differential equations for these parameters. These ODEs may then be studied to determine if the amplitude of the resulting wave packet might grow to become sufficiently large to constitute something like a rogue wave.

We use the parameterisation (29) with the length of the wave $L(t)$ and the amplitude, $A(t)$, related by the energy condition (30), and the initial amplitude A_0 and the initial length, L_0.

Following the ideas of Cousins [2] we can multiply (26) through by a weight function (they use a sech function) and integrate the resulting equation $\int_{-\infty}^{\infty}(..)\,\mathrm{sech}x\ \mathrm{d}x$, and hence obtain the amplitude equation to determine the growth of a wave as

$$\frac{\mathrm{d}^2|A|^2}{\mathrm{d}t^2} = \frac{K}{|A|^2}\left(\frac{\mathrm{d}|A|^2}{\mathrm{d}t}\right)^2 + \frac{3|A|^2(2|A|^2L^2-1)}{64L^2} \tag{31}$$

where $K = (3\pi^2 - 16)/8$. Equation (31) along with the constraint (30) could be solved numerically (say), subject to initial conditions. We know that

$$|A(0)|^2 = A_0^2 \quad \text{at } t = 0, \tag{32}$$

but (31) requires a second condition so we might adopt

$$\frac{\mathrm{d}|A|}{\mathrm{d}t} = 0 \quad \text{at } t = 0. \tag{33}$$

2.3 Phase-plane analysis of NLSE

The problem defined by (31) and (30) can be reduced to a 2nd-order ODE by letting $Y = |A|^2$, so that

$$\frac{\mathrm{d}^2Y}{\mathrm{d}t^2} = \frac{K}{Y}\left(\frac{\mathrm{d}Y}{\mathrm{d}t}\right)^2 + \frac{3Y^2\,A_0^2(2L_0^2\,A_0^2 - Y)}{64L_0^2\,A_0^4}. \tag{34}$$

Rescaling with the expressions,

$$Y = (L_0^2\,A_0^2)y = \frac{y}{4A_0^2} \quad \text{and} \quad t = (L_0\,A_0^2)^{-1}\tau = 2\tau \tag{35}$$

reduces equation (34) to

$$\frac{\mathrm{d}^2y}{\mathrm{d}\tau^2} = \frac{K}{y}\left(\frac{\mathrm{d}y}{\mathrm{d}\tau}\right)^2 + \frac{3}{64}y^2(2-y) \tag{36}$$

Finally, letting

$$\frac{\mathrm{d}y}{\mathrm{d}\tau} = z \tag{37}$$

$$\frac{\mathrm{d}z}{\mathrm{d}\tau} = \frac{Kz^2}{y} + \frac{3}{64}y^2(2-y) \tag{38}$$

and dividing (38) by (37) provides the ODE

$$\frac{\mathrm{d}z}{\mathrm{d}y} = \frac{Kz}{y} + \frac{3}{64}\frac{y^2(2-y)}{z} \tag{39}$$

Using initial conditions and putting everything in terms of A_0,

$$y(0) = \frac{1}{L_0^2\,A_0^2} = 4A_0^2 \tag{40}$$

$$\dot{y}(0) = z(0) = 0 \tag{41}$$

we can draw trajectories in the (y, z) phase-plane for different cases. The fixed point location $y = 2, z = 0$ corresponds to $A_0 = 1/\sqrt{2}$, the value for the original, exact soliton solution.

The phase-plane portraits are shown in Figure 6, which shows a close-up of the region about $y = 2$ and Figure 7, which pans out to show what happens for larger values of z. It seems that all trajectories return to $z = 0$ eventually at $y > 2$, which corresponds to larger values of A.

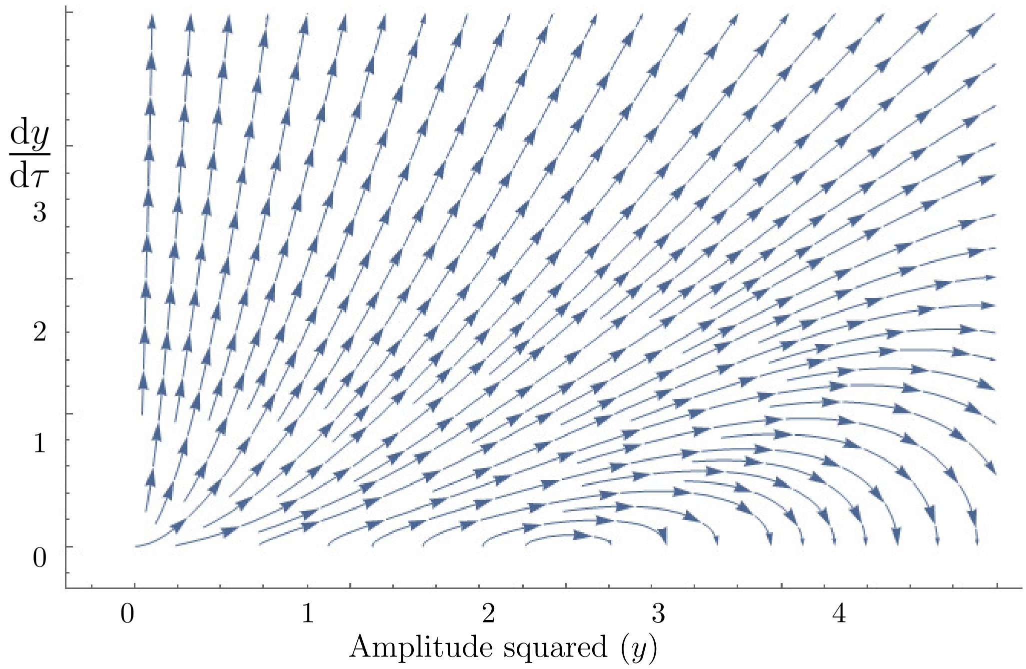

Figure 6: Phase plot of $z = \frac{dy}{d\tau}$ vs. y showing $0 < \frac{dy}{d\tau} < 4.25$. Trajectories that start with $y < 2$ but close to $y \sim 2$ appear to return to $z = 0$ relatively quickly.

The initial conditions and behaviours fall within the ranges;

$$\text{if } y(0) < 2, \quad \Rightarrow A_0 < \frac{1}{\sqrt{2}} \text{ then the amplitude grows, while}$$
$$\text{if } y(0) > 2, \quad \Rightarrow A_0 > \frac{1}{\sqrt{2}} \text{ then the amplitude stays the same.}$$

For example, the case in which $y(0) \approx 1.34$ $(A_0 \approx 0.58)$ travels toward $y \to 3$ $(A \to 0.87)$, while that which starts at $y(0) \approx 0.5$ $(A_0 \approx 0.35)$ approaches $y \to 14$ $(A \to 1.87)$. Recall that $\sqrt{2} \approx 0.7071$ and so this is around 2.5 times the amplitude of the original soliton.

In other words, if the starting condition is such that $A_0 > 1/\sqrt{2}$, then the wave is at the end of its trajectory and so will remain there, i.e. nothing will happen and the soliton will propagate with constant amplitude in a kind of steady solution. If the starting condition is such that $A_0 < 1/\sqrt{2}$, then the value of z, i.e. $\frac{dy}{d\tau}$ will increase so that either the amplitude increases and the wavelength decreases until as $\tau \to \infty$ the wave becomes a steady, steeper soliton propagating forward. Recall that in dimensional terms, $|A|^2$ scales

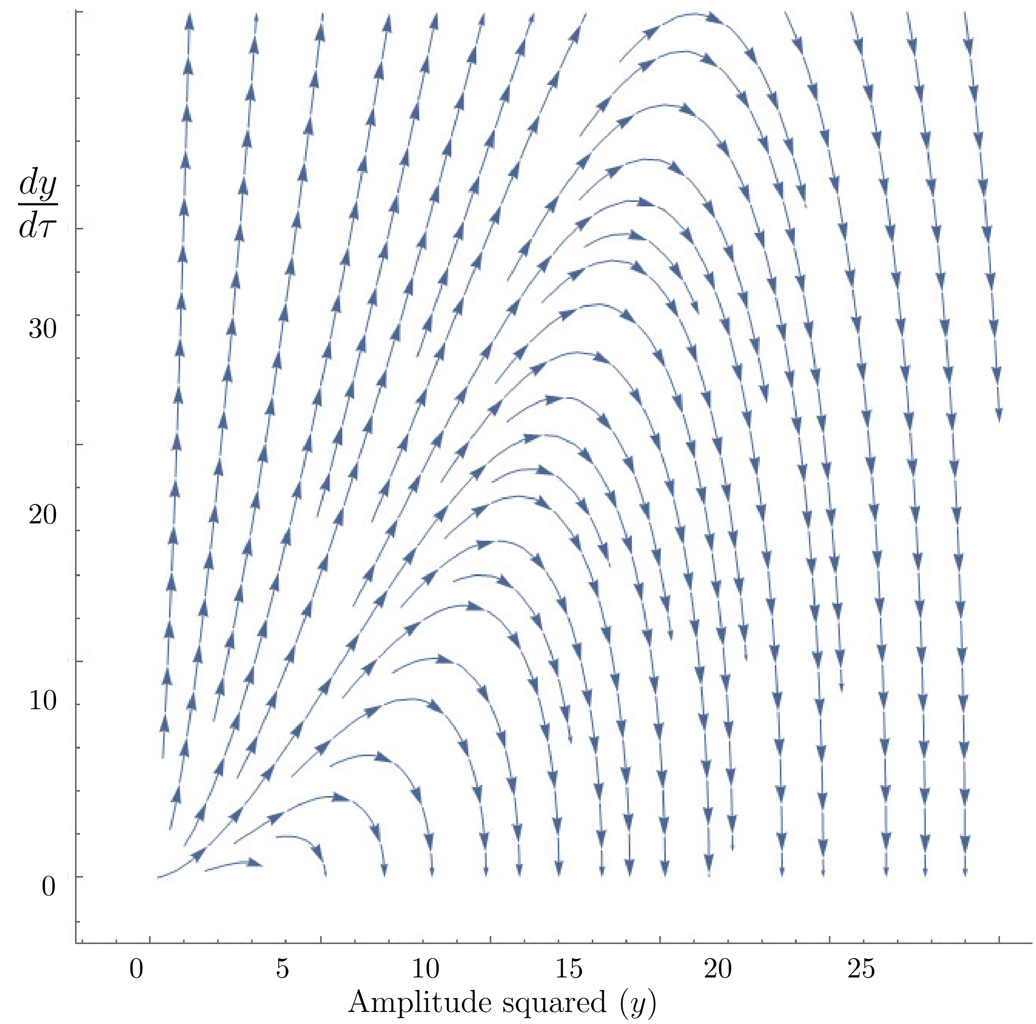

Figure 7: Phase plot of $z = \frac{\mathrm{d}y}{\mathrm{d}\tau}$ vs. y over a large region of phase space. This view shows that the trajectories all eventually return to $z = \frac{\mathrm{d}y}{\mathrm{d}\tau} = 0$, which would correspond to a relatively small wave.

with k^4a^2, where k is our original wavenumber and a is our original amplitude, with the expectation that $1/k >> a$. The timescale in the phase portrait in dimensional terms is $(k^{3/2}ag^{1/2})^{-1}$, which is very long. It does appear that small solitons could potentially grow to large waves given sufficient time. However, we must remember that this analysis is based on assuming that this wave packet has small variations from the soliton solution and so for the largest waves to occur this variation would need to be quite significant.

3 Comments

There is a vast literature on the possible mechanisms for the generation of rogue waves. The NLSE and its variants is but one of a number of equations that might be used to develop a model. A study of these papers would provide a greater insight into how appropriate they are to this particular problem. It seems that there is some potential for these equations to generate such waves, but it is not clear from these models how they could be used to predict when and where they might form. The work of Dysthe et. al. [4] gives a more comprehensive discussion of rogue wave formation and we recommend the reader to this review. Their considerations include not only the mechanisms discussed herein, but also refractive focussing due to topographical effects in the presence of strong currents.

We mapped the location of rogue waves picked up in recent years to see if there was any indicator of a cause, but without success, there being no apparent correlation between the locations and sea conditions that might indicate a consistent cause via the sea currents, wind behaviour or bottom topography. No doubt a more detailed analysis of the location at which such waves have been recorded would assist in deciding whether some other factors were required to generate the waves, or whether it is a nonlinear interaction as proposed in the analysis given above.

In this workshop, it was not possible to examine all of the existing work on this subject, and so we considered in some detail the derivation of one possible mechanism using the NLSE equation. This analysis did raise the possibility of nonlinear interactions being the cause of the waves, but if that is the case then mapping sea conditions in order to predict the formation would be extremely difficult as they form over a very long time scale.

References

[1] EM Bitner-Gregersen, L Fernandez, JM Lefèvre, J Monbaliu and A Toffoli. The North Sea Andrea storm and numerical simulations, *Natural Hazards and Earth System Sciences*, **14** (2014), 1407-1415.

[2] W Cousins and TP Sapsis. Unsteady evolution of localized unidirectional deep-water wave groups. *Phys. Rev. E*, **91** (2015), 063204.

[3] KB Dysthe. Note on a modification to the nonlinear Schrodinger equation for application to deep water waves. *Proc. R. Soc. Lond. A*, **369**, (1979), 105-114

[4] KB Dysthe, HE Krogstad and P Müller. Oceanic Rogue Waves. *Ann. Rev. Fluid Mech.*, **40**, (2008), 287-310.

[5] ML McAllister, S Draycott, TA Adcock, PH Taylor and TS van den Bremer. Laboratory recreation of the Draupner wave and the role of breaking in crossing seas, *J. Fluid Mech.*, **860**, (2019), 767-786.

[6] Anonymous. List of Rogue Waves.
`https://en.wikipedia.org/wiki/List_of_rogue_waves`

[7] windy.com. Ocean currents.
`https://www.windy.com`